

Article

## Regulation of the Spontaneous Augmentation of $\text{Na}_v1.9$ in Mouse Dorsal Root Ganglion Neurons: Effect of PKA and PKC Pathways

Jun-ichi Kakimura <sup>1,2,\*</sup>, Taixing Zheng <sup>2</sup>, Noriko Uryu <sup>2</sup> and Nobukuni Ogata <sup>2</sup>

<sup>1</sup> Technical Center, Hiroshima University, Hiroshima, 734-8551, Japan

<sup>2</sup> Department of Neurophysiology, Graduate School of Biomedical Sciences, Hiroshima University, Hiroshima, 734-8551, Japan; E-Mails: tei0322@hiroshima-u.ac.jp (T.Z.); uryu@asahi.ac.jp (N.U.); ogatan@hiroshima-u.ac.jp (N.O.)

\* Author to whom correspondence should be addressed; E-Mail: kakimura@hiroshima-u.ac.jp; Tel.: +81-82-257-5127; Fax: +81-82-257-5127.

Received: 15 January 2010; in revised form: 8 February 2010 / Accepted: 18 March 2010 /

Published: 19 March 2010

---

**Abstract:** Sensory neurons in the dorsal root ganglion express two kinds of tetrodotoxin resistant (TTX-R) isoforms of voltage-gated sodium channels,  $\text{Na}_v1.8$  and  $\text{Na}_v1.9$ . These isoforms play key roles in the pathophysiology of chronic pain. Of special interest is  $\text{Na}_v1.9$ : our previous studies revealed a unique property of the  $\text{Na}_v1.9$  current, *i.e.*, the  $\text{Na}_v1.9$  current shows a gradual and notable up-regulation of the peak amplitude during recording (“spontaneous augmentation of  $\text{Na}_v1.9$ ”). However, the mechanism underlying the spontaneous augmentation of  $\text{Na}_v1.9$  is still unclear. In this study, we examined the effects of protein kinases A and C (PKA and PKC), on the spontaneous augmentation of  $\text{Na}_v1.9$ . The spontaneous augmentation of the  $\text{Na}_v1.9$  current was significantly suppressed by activation of PKA, whereas activation of PKA did not affect the voltage dependence of inactivation for the  $\text{Na}_v1.9$  current. On the contrary, the finding that activation of PKC can affect the voltage dependence of inactivation for  $\text{Na}_v1.9$  in the perforated patch recordings, where the augmentation does not occur, suggests that the effects of PMA are independent of the augmentation process. These results indicate that the spontaneous augmentation of  $\text{Na}_v1.9$  was regulated directly by PKA, and indirectly by PKC.

**Keywords:**  $\text{Na}^+$  channel; tetrodotoxin; dorsal root ganglion; patch clamp; PKA; PKC

---

## 1. Introduction

Voltage-gated sodium channels ( $\text{Na}^+$  channels) mediate the transient increase in  $\text{Na}^+$  conductance that underlies the action potential of neurons and other excitable cells. In mammals, a family of  $\text{Na}^+$  channel  $\alpha$  subunits (designated  $\text{Na}_v1.1$ - $\text{Na}_v1.9$ ) exhibit unique patterns of anatomical expression and varied functional and pharmacological properties [1,2].

Unmyelinated C-fibers originate from small primary afferent neurons of the dorsal root ganglion (DRG), and transmit nociceptive information to the central nervous system.  $\text{Na}^+$  currents expressed in small DRG neurons can be classified into two categories on the basis of their relative sensitivity to tetrodotoxin (TTX); the first, TTX-sensitive (TTX-S)  $\text{Na}^+$  currents and the second, TTX-resistant (TTX-R)  $\text{Na}^+$  currents. TTX-R  $\text{Na}^+$  currents can be further subdivided into the current mediated by  $\text{Na}_v1.8$ , known as SNS [3–6], and the current mediated by  $\text{Na}_v1.9$ , known as NaN [7–11].

The  $\text{Na}_v1.9$  current is characterized by a low activation threshold of about -60 mV and the depolarized steady-state inactivation ( $h_\infty$ ) curve [7,11–13]. From these observations, the  $\text{Na}_v1.9$  current may mainly regulate subthreshold excitability of small DRG neurons [7,10,11,13]. Our previous studies have demonstrated gradual and notable increase-decrease of the peak amplitude of the  $\text{Na}_v1.9$  current during whole-cell patch clamp recording (referred to as ‘spontaneous augmentation of  $\text{Na}_v1.9$ ’). The spontaneous augmentation of  $\text{Na}_v1.9$  was not observed in the presence intracellular ATP (3 mM) and by using nystatin-perforated patch clamp recording. These results suggest possible involvement of the intracellular environment in the spontaneous augmentation of  $\text{Na}_v1.9$  [11].

It is well known that protein kinases A and C (PKA and PKC), and phosphatases, as well as other proteins such as  $\text{Ca}^{2+}$ -calmodulin-dependent kinase, growth-factor-dependent receptor tyrosine kinases, extracellular signal-regulated kinases and heterotrimeric G proteins, also modulate  $\text{Na}^+$  channels [14–16]. At present, endogenous factors that regulate the spontaneous augmentation of  $\text{Na}_v1.9$  have not been identified. In sensory neurons, activation of PKA and PKC affects the biophysical properties of  $\text{Na}^+$  channels [1]. As a first step to the above issue, we focused on the possible involvement of the PKA and PKC pathways in the spontaneous augmentation of  $\text{Na}_v1.9$ . For this purpose, in this study we examined the effects of activators and inhibitors of PKA and PKC on the spontaneous augmentation of  $\text{Na}_v1.9$ , using  $\text{Na}_v1.8$  knock-out (KO) mice [5,11,13] to record the  $\text{Na}_v1.9$  current in isolation.

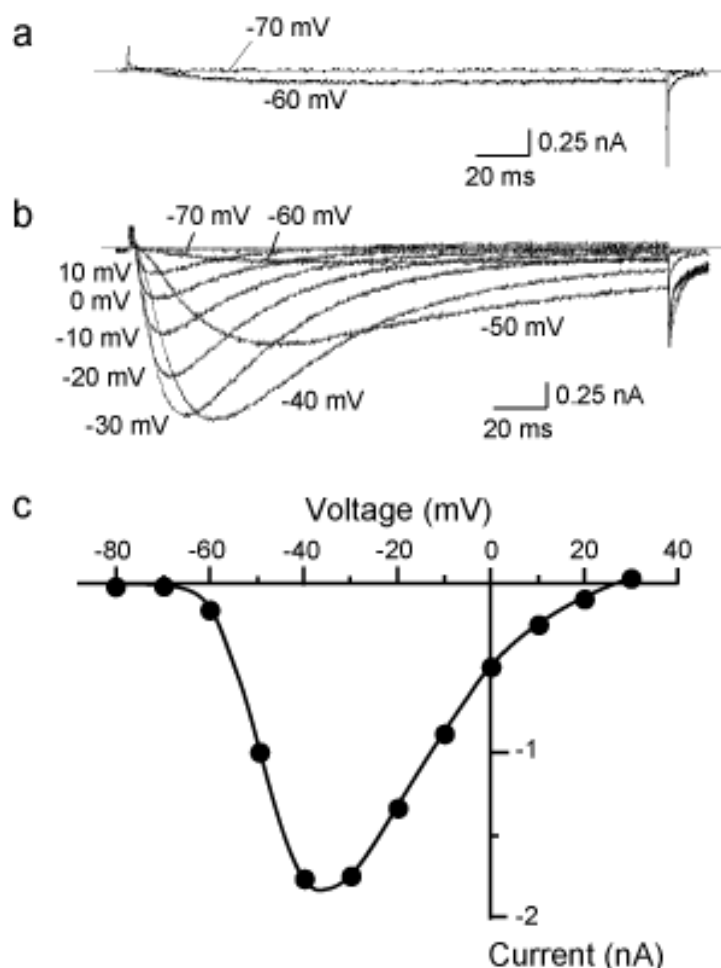
## 2. Results and Discussion

### 2.1. Characterization of the $\text{Na}_v1.9$ current

The detailed properties of the  $\text{Na}_v1.9$  current was already described in our previous reports [11,13,17]. A typical example of the  $\text{Na}_v1.9$  currents is shown in Figure 1. Currents were evoked by a 200 ms test pulse ( $V_T$ ) from a holding potential ( $V_H$ ) of -80 mV. TTX-sensitive (TTX-S)  $\text{Na}^+$  currents were completely eliminated by 200 nM TTX contained in the external solution. The  $\text{Na}_v1.9$  current had an activation threshold at about -60 mV (Figure 1a), which was more negative than thresholds for  $\text{Na}^+$  currents mediated by  $\text{Na}_v1.8$  and other TTX-S  $\text{Na}^+$  currents (about -40 mV) [13]. Time courses of activation and inactivation of the  $\text{Na}_v1.9$  current were extremely prolonged, particularly at lower

activation voltages (Figure 1b). Figure 1c illustrates the current-voltage relationship for the currents shown in Figure 1b.

**Figure 1.** Typical examples of the tetrodotoxin-resistant (TTX-R)  $\text{Na}^+$  current mediated by  $\text{Na}_v1.9$ . The  $\text{Na}_v1.9$  current was recorded from the small (diameter  $< 25 \mu\text{m}$ ) dorsal root ganglion (DRG) neuron prepared from the  $\text{Na}_v1.8$  knock-out (KO) mouse. Currents were elicited by 200 ms test pulse ( $V_T$ ) from a holding potential ( $V_H$ ) of  $-80 \text{ mV}$ . (a) The activation threshold for the  $\text{Na}_v1.9$  current. The  $\text{Na}_v1.9$  current could be activated at  $-60 \text{ mV}$ , whereas  $V_T$  to  $-70 \text{ mV}$  failed to elicit. (b) A family of superimposed  $\text{Na}_v1.9$  currents evoked by  $V_{TS}$  between  $-70$  and  $+10 \text{ mV}$  in  $10\text{-mV}$  increments from  $V_H$  of  $-80 \text{ mV}$ . The external solution contained  $200 \text{ nM}$  TTX. Voltage labels attached to traces indicate  $V_{TS}$ . (c) The current-voltage curve for the  $\text{Na}_v1.9$  current shown in panel (b). Peak amplitudes of the currents were plotted against  $V_T$ .



## 2.2. Modification of the spontaneous augmentation of $\text{Na}_v1.9$ by PKA and PKC

As previously described [11,17], the peak amplitude of the  $\text{Na}_v1.9$  current remarkably increased during conventional whole-cell recording with control pipette solution. As shown in Figure 2, the peak amplitude of the  $\text{Na}_v1.9$  current gradually increased up to  $18.7 \pm 5.0$ -fold of the initial value ( $n = 10$ ), and then diminished towards the initial value. The total duration of the spontaneous augmentation of

$\text{Na}_V1.9$  was  $12.4 \pm 1.7$  min ( $n = 10$ ). In addition, activation and inactivation kinetics of this current did not change during the spontaneous augmentation of  $\text{Na}_V1.9$  (Figure 2c).

**Figure 2.** (a) Time courses of the  $\text{Na}_V1.9$  currents recorded with normal pipette solution. The  $\text{Na}_V1.9$  current was evoked by  $V_T$  to  $-10$  mV from  $V_H$  of  $-80$  mV, and command pulses were applied every 30 s. Then, selected traces were superimposed. (b) Typical example of the spontaneous augmentation of  $\text{Na}_V1.9$ . Peak amplitudes of the  $\text{Na}_V1.9$  current were plotted as a function of time after onset of the spontaneous augmentation of  $\text{Na}_V1.9$ . Numbers indicate the traces shown in panel (a). (c) Traces of the  $\text{Na}_V1.9$  currents shown in panel (a) were normalized and then superimposed. (d) Time courses of the  $\text{Na}_V1.9$  currents in all cases examined.

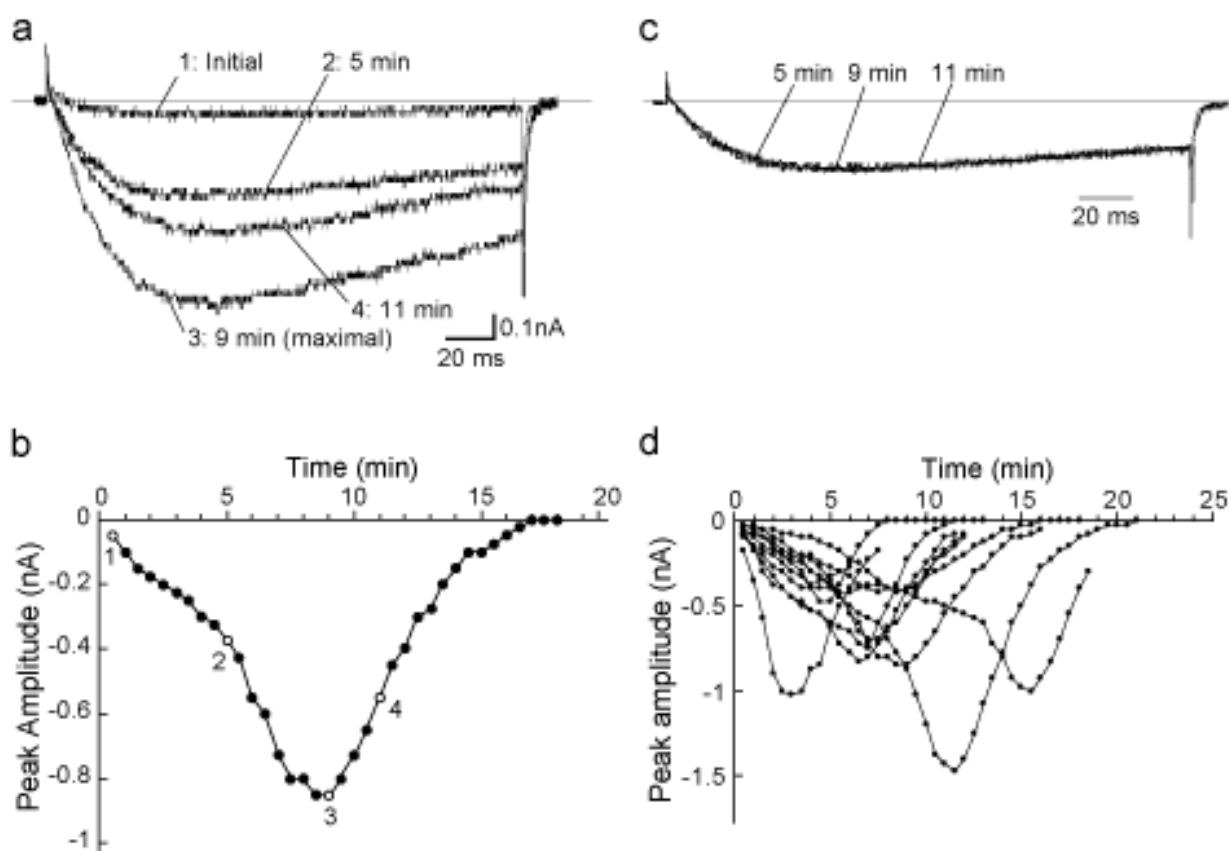
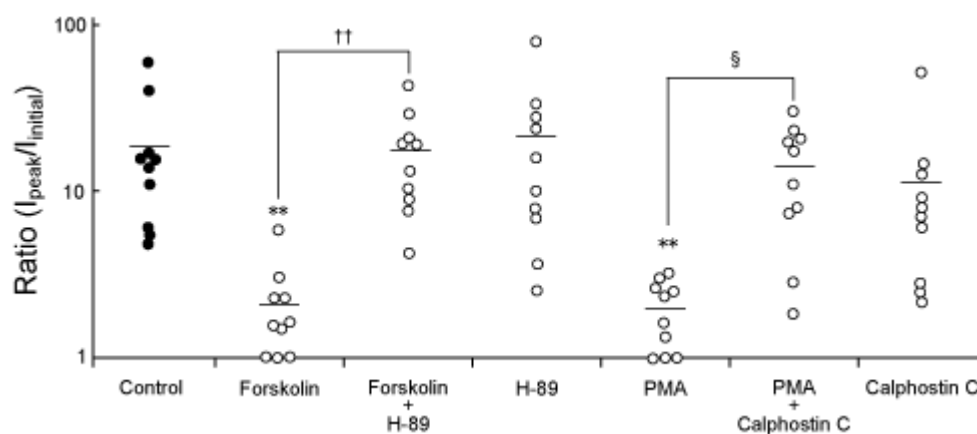


Figure 3 summarizes the intensity changes of the spontaneous augmentation of  $\text{Na}_V1.9$ , which were induced by compounds added to the pipette solution. In the presence of a PKA activator, forskolin ( $10 \mu\text{M}$ ), the intensity of the spontaneous augmentation of  $\text{Na}_V1.9$  was significantly attenuated ( $2.1 \pm 0.5$ -fold:  $n = 10$ ). Although a PKA inhibitor, H-89 ( $10 \mu\text{M}$ ), alone had no detectable effect on the intensity of the spontaneous augmentation of  $\text{Na}_V1.9$  ( $21.1 \pm 7.3$ -fold:  $n = 10$ ), the effect of forskolin was significantly inhibited by treatment with H-89 ( $17.3 \pm 3.5$ -fold:  $n = 10$ ). A PKC activator, PMA ( $100 \text{ nM}$ ), had significant suppressive effect on the intensity of the augmentation of  $\text{Na}_V1.9$  ( $2.0 \pm 0.3$ -fold:  $n = 10$ ). In the presence of a PKC inhibitor, calphostin C ( $100 \text{ nM}$ ), the effect of PMA on the augmentation of  $\text{Na}_V1.9$  was significantly inhibited ( $14.2 \pm 2.8$ -fold:  $n = 10$ ). Similarly to H-89, calphostin C alone had no discernable effect on the spontaneous augmentation of  $\text{Na}_V1.9$  ( $11.3 \pm 4.4$ -fold:  $n = 10$ ).

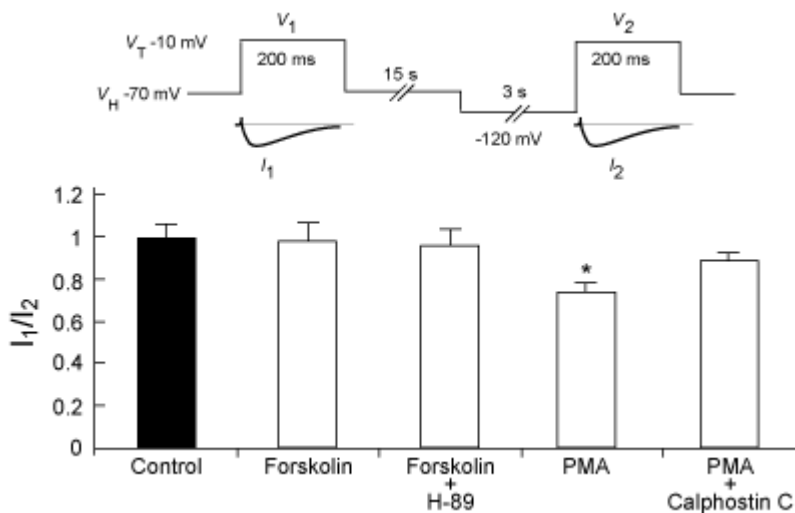
**Figure 3.** Modification of the spontaneous augmentation of  $\text{Na}_V1.9$  by addition of the PKA activator forskolin and the PKC activator PMA to the pipette solution. The ordinate shows the ratio of maximal amplitude during recording to the initial amplitude of the  $\text{Na}_V1.9$  current ( $I_{\text{maximal}}/I_{\text{initial}}$ ). A ratio  $> 1$  indicates the occurrence of the spontaneous augmentation of  $\text{Na}_V1.9$ , whereas a ratio  $= 1$  indicates no change or reduction of the peak amplitude of the  $\text{Na}_V1.9$  current. The plots are shown on a logarithmic scale. Circles indicate the ratios obtained for individual trials. Filled circles, control; open circles, treated groups. Horizontal bars indicate the mean values of each group.  $**P < 0.01$  versus control,  $\dagger\dagger P < 0.01$  versus forskolin, and  $\S P < 0.05$  versus PMA.



### 2.3. Possible involvement of PKA and PKC pathways in the voltage dependence of inactivation for the $\text{Na}_V1.9$ current

We next examined the effects of forskolin and PMA on the voltage dependence of inactivation for the  $\text{Na}_V1.9$  current (Figure 4). The voltage dependence of inactivation was determined by measuring peak amplitudes of the  $\text{Na}_V1.9$  currents evoked by  $V_T$  to  $-10$  mV from  $V_{HS}$  of  $-70$  mV ( $I_1$ ) and  $-120$  mV ( $I_2$ ) intermittently (every 1 minute), and then the ratio of  $I_1/I_2$  obtained from each group was compared. Just after commencing recording, there were no significant differences between each group (data not shown). 10 minutes after commencing recording, the presence of forskolin ( $10 \mu\text{M}$ ) alone, or the co-presence of forskolin and H-89 ( $10 \mu\text{M}$ ), did not significantly change the ratios of  $I_1/I_2$  ( $1.00 \pm 0.08$ :  $n = 8$ , and  $0.99 \pm 0.06$ :  $n = 6$ , respectively) versus control ( $0.99 \pm 0.07$ :  $n = 8$ ). On the contrary,  $100$  nM PMA significantly reduced the ratio of  $I_1/I_2$  ( $0.75 \pm 0.07$ :  $n = 8$ ) as compared to control. Calphostin C ( $100$  nM) inhibited PMA-induced reduction of  $I_1/I_2$  ( $0.91 \pm 0.03$ :  $n = 5$ ).

**Figure 4.** The change of the voltage-dependence of inactivation for the  $\text{Na}_V1.9$  current by activation of PKC. The  $\text{Na}_V1.9$  currents were evoked by the pulse protocol shown in the diagram. We previously confirmed that the duration of  $V_H$  for 3 s was sufficient to achieve steady state availability for  $\text{Na}_V1.9$  [11]. Peak amplitudes of the  $\text{Na}_V1.9$  currents ( $I_1$  and  $I_2$ ) were monitored for 10 min after commencing recording, and the resulting  $I_1/I_2$  ratios were compared. \* $P < 0.05$  versus control.



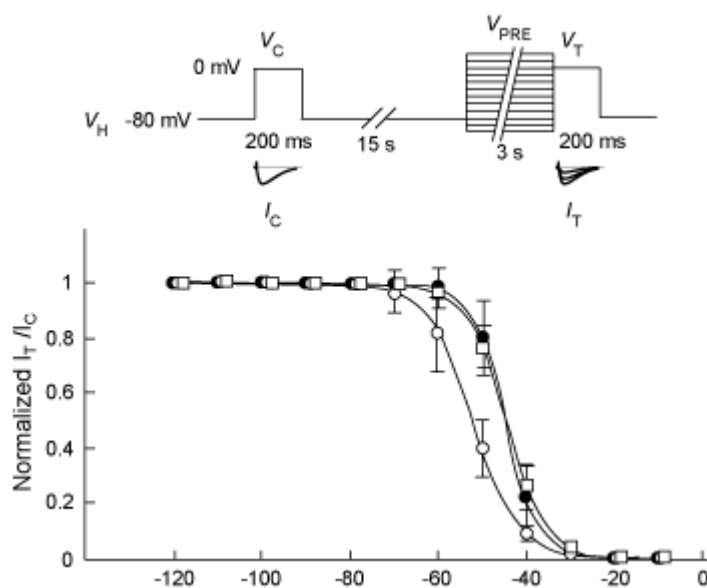
#### 2.4. The effect of PMA on the $h_\infty$ curve for the $\text{Na}_V1.9$ current is reproducible under nystatin-perforated patch clamp recording

The spontaneous augmentation of  $\text{Na}_V1.9$  was prevented by using nystatin-perforated patch clamp recording [11]. Therefore, we further examined the effect of forskolin and PMA on the  $h_\infty$  (voltage dependence of steady-state inactivation) curve for the  $\text{Na}_V1.9$  current in such a situation. The  $\text{Na}_V1.9$  current was evoked by  $V_T$  to 0 mV after various  $V_{\text{PRES}}$  steps ranging from -120 mV to 10 mV in 10-mV steps for 3 s (see diagram of Figure 5). Figure 5 shows  $h_\infty$  curves for the  $\text{Na}_V1.9$  current before (control) and after application of 100 nM PMA or 10  $\mu\text{M}$  forskolin for 10 min. The  $h_\infty$  curves were fitted to the Boltzmann equation:

$$I/I_{\text{max}} = 1/\{1+\exp[(V_{\text{PRE}}-V_{1/2})/k]\} \quad (1)$$

Where  $I$  is the peak amplitude of the  $\text{Na}_V1.9$  current obtained by  $V_T$ ,  $I_{\text{max}}$  is the peak amplitude of the  $\text{Na}_V1.9$  current evoked by  $V_C$ ,  $V_{1/2}$  is the half-maximum inactivation voltage, and  $k$  is the slope factor. We found significant differences ( $P < 0.05$ ) between parameters obtained after PMA application ( $n = 5$ ,  $V_{1/2} = -52.1 \pm 5.4$  mV,  $k = 5.17 \pm 0.44$  mV) versus control ( $n = 4$ ,  $V_{1/2} = -44.7 \pm 6.4$  mV,  $k = 3.75 \pm 0.15$  mV). On the contrary, there was no significant change between values obtained after forskolin application ( $n = 5$ ,  $V_{1/2} = -44.6 \pm 2.1$  mV,  $k = 4.44 \pm 0.51$  mV) from the control.

**Figure 5.** The  $h_\infty$  curve for the  $\text{Na}_V1.9$  current under nystatin-perforated patch clamp recording. The diagram illustrates the pulse protocol. Two identical pulses to 0 mV for 200 ms were applied 15 s prior ( $V_C$ ) and immediately subsequent ( $V_T$ ) to the conditioning pre-pulse ( $V_{PRE}$ ) of -120 to 10 mV for 3 s from  $V_H$  of -80 mV.  $V_C$  was delivered to minimize the error arising from possible fluctuation of the current (see experimental section). The pulse protocol was applied every 40 s. The peak amplitude of the current ( $I_T$ ) evoked by  $V_T$  was divided by the peak amplitude of the current ( $I_C$ ) evoked by  $V_C$ . The ratio of  $I_T/I_C$  was normalized and plotted against  $V_{PRE}$ . The  $h_\infty$  curve for  $\text{Na}_V1.9$  current was determined, before (control, filled circle) and 10 min after bath application of PMA (open circle) or forskolin (open square).



## 2.5. Discussion

The expression of the  $\text{Na}_V1.9$  current is confined to the subpopulation of primary afferent neurons with a small cell-body diameter similarly to the  $\text{Na}_V1.8$  current [4–8,10,11,18]. This observation suggests that  $\text{Na}_V1.9$  plays an important role in nociception, similar to  $\text{Na}_V1.8$ . On the other hand, the electrophysiological properties of the  $\text{Na}_V1.9$  current differ notably from those of the  $\text{Na}_V1.8$  current, *i.e.*, the  $\text{Na}_V1.9$  current has a more hyperpolarized activation threshold, much slower activation and inactivation kinetics, and a more depolarized  $h_\infty$  curve [11,13]. These observations suggest that the role of  $\text{Na}_V1.9$  in nociception may be distinct from that of  $\text{Na}_V1.8$ .

It was reported that the sustained membrane depolarization (over several hundreds of milliseconds), which is resistant to TTX, is observed in myenteric ganglia [12]. In addition, we previously observed similar sustained membrane depolarization mediated by  $\text{Na}_V1.9$  in small DRG neurons [13]. The  $\text{Na}_V1.9$  current may have facilitatory functions in the generation of action potential. On the other hand,  $h_\infty$  curves for other  $\text{Na}^+$  currents are more depolarized than that of  $\text{Na}_V1.9$  [11,13]. Taking into consideration these properties, sustained activation of  $\text{Na}_V1.9$  may decrease the availability of other  $\text{Na}^+$  channels, and then conversely act to inhibit generation of action potential. Thus, the regulation of membrane potential by  $\text{Na}_V1.9$  may be facilitatory or inhibitory to generating an action potential, in a context-dependent manner.

In addition, we observed a sporadic and remarkable increase of the peak amplitude of the  $\text{Na}_v1.9$  current followed by decrease of the peak amplitude during whole-cell patch clamp recording (“spontaneous augmentation of  $\text{Na}_v1.9$ ”) [11]. We previously reported that the spontaneous augmentation of  $\text{Na}_v1.9$  was inhibited by recording with the nystatin-perforated patch clamp technique, and in the presence of intracellular ATP [11,17]. These results suggest a possible involvement of the intracellular environment in the spontaneous augmentation of  $\text{Na}_v1.9$ .

Analyses of brain  $\text{Na}^+$  channels have shown that the cytoplasmic loop between domains DI and DII of  $\text{Na}^+$  channels possesses several shared PKA and PKC phosphorylation sites [19–20]. In addition, the inactivation gate has a unique site for PKC phosphorylation [22,23]. In fact, activation of PKA reduces the peak amplitude of brain  $\text{Na}^+$  channels without the shift of the steady-state properties [20,24]. On the other hand, activation of PKC has regulatory effects on skeletal muscle  $\text{Na}^+$  channels [25], brain  $\text{Na}^+$  channels [26] and peripheral nerve  $\text{Na}^+$  channel expressed in *Xenopus* oocytes [27]. However, the effects of PKA and PKC on the spontaneous augmentation of  $\text{Na}_v1.9$  in sensory neurons have not been investigated.

First, we focused on the effect of PKA on the spontaneous augmentation of  $\text{Na}_v1.9$ . The spontaneous augmentation of  $\text{Na}_v1.9$  was significantly suppressed in the presence of forskolin, and H-89 significantly inhibited this suppressive effect of forskolin (Figure 3). These results indicate that the spontaneous augmentation of  $\text{Na}_v1.9$  is suppressed by activation of PKA. It is well known that the amplitude of  $\text{Na}^+$  current is strongly affected by steady-state inactivation of the channel. However, forskolin did not change the  $h_\infty$  curve parameters for the  $\text{Na}_v1.9$  current in comparison with the control (Figures 4 and 5). This suggests that inhibition of the spontaneous augmentation of  $\text{Na}_v1.9$  by PKA activation was not due to the hyperpolarizing shift of the  $h_\infty$  curve for the  $\text{Na}_v1.9$  current.

Next, we focused on the effect of PKC on the spontaneous augmentation of  $\text{Na}_v1.9$ . PMA significantly reduced the intensity of augmentation, and the effect of PMA was significantly suppressed by Calphostin C (Figure 3). However, application of PMA induced the hyperpolarizing shift of the voltage dependence of inactivation for the  $\text{Na}_v1.9$  current. Thus, apparent suppression of the spontaneous augmentation of  $\text{Na}_v1.9$  by PMA was largely due to hyperpolarizing shift of the  $h_\infty$  curve for the  $\text{Na}_v1.9$  current.

A similar phenomenon has also been reported by Baker *et al.*, who showed that intracellular GTP [28] or activation of PKC [29] induces the up-regulation of the  $\text{Na}_v1.9$  current. There are distinct dissimilarities between the up-regulation reported by Baker *et al.* and the spontaneous augmentation of  $\text{Na}_v1.9$  described in the present study and also in our previous reports [11,13,17]. Namely, (1) the up-regulation reported by Baker *et al.* was observed in the presence of intracellular ATP. On the contrary, the spontaneous augmentation of  $\text{Na}_v1.9$  in our experiments occurred only in the absence of intracellular ATP. (2) the up-regulation reported by Baker *et al.* was mediated by intracellular GTP or activation of PKC. On the other hand, we find that intracellular GTP has no effect on the spontaneous augmentation of  $\text{Na}_v1.9$  (unpublished data). (3) Baker *et al.* showed only an increment of peak amplitude of the  $\text{Na}_v1.9$  current, and did not show the entire time course of the phenomenon [28,29]. The spontaneous augmentation of  $\text{Na}_v1.9$  was composed of an increase and a subsequent decrease of peak amplitude of the  $\text{Na}_v1.9$  current. From these observations, the up-regulation reported by Baker *et al.* may be distinct from the spontaneous augmentation of  $\text{Na}_v1.9$  in our studies.

A recent behavioral study showed that the PKA inhibitor, H-89, suppresses bee venom-induced mechanical hyperalgesia in rats [30], and the activation of PKA is conducive to the inflammatory mechanical hyperalgesia [31,32]. In addition, activity of specific PKC isozymes is increased in inflammatory-pain models in rats [33–36]. From these observations, the  $\text{Na}_v1.9$  channel may be regulated not to increase the amplitude of the  $\text{Na}_v1.9$  current, *i.e.*, the spontaneous augmentation of  $\text{Na}_v1.9$  under pathological condition by PKA and/or PKC activation.

Recently, it has been reported that  $\text{Na}_v1.9$  underlies nociceptive behavior after peripheral inflammation in  $\text{Na}_v1.9$  KO mice [37]. In addition, histochemical study on  $\text{Na}_v1.9$  channel proteins in axons of normal and complete Freund's adjuvant-inflamed rats showed significant decrease of the proportion of  $\text{Na}_v1.9$ -labeled unmyelinated axons, and no change in the proportion of labeled myelinated axons following inflammation [18]. Taken together, the  $\text{Na}_v1.9$  current contributes to pain signaling, and may alter under pathophysiological conditions.

### 3. Experimental Section

#### 3.1. Isolation of single DRG neurons and cell culture

The protocols were approved by Hiroshima University Animal Ethics Committee. Dissociation of single DRG neurons and their culture was described previously. [11,13]. Briefly, adult mice were sacrificed by cervical dislocation under ethylcarbamate anesthesia (3 mg/g; Wako Pure Chemicals, Osaka, Japan). DRGs from all segments of the spinal cord were dissected from  $\text{Na}_v1.8$  KO mice [5] and desheathed in ice-cold  $\text{Ca}^{2+}/\text{Mg}^{2+}$ -free phosphate-buffered saline (PBS(-)). The isolated DRGs were incubated sequentially in PBS(-) containing 0.2% collagenase (Wako Pure Chemicals) and 0.1% trypsin (Sigma, St. Louis, Mo., USA), each for 20 min at 37 °C. DRGs were then dissociated by trituration with fire-polished Pasteur pipettes in culture medium composed of Dulbecco's modified Eagle medium 10% (vol./vol.) heat-inactivated fetal calf serum.

The dissociated cells were plated on 35 mm plastic tissue-culture dishes pre-coated with 0.01% poly-L-lysine (Sigma) and maintained in culture medium supplemented with penicillin (100 IU/mL) and streptomycin (100 µg/mL). All cultured cells were maintained at 37 °C in 5%  $\text{CO}_2/95\%$  air. Cells were used for experiments after short-term culture (4–12 h after plating). At this time in culture, neurite outgrowth was not observed. We defined DRG neurons that were smaller than 25 µm in diameter as small neurons [13,28], and small neurons thus defined were used throughout the study.

#### 3.2. Electrophysiology

Voltage clamp recordings were performed using an Axopatch 200A amplifier (Axon Instruments, Union City, CA, USA). The  $\text{Na}^+$  currents were recorded by using either the conventional whole-cell patch clamp technique [38] or the nystatin-perforated patch clamp technique [39] at room temperature (22–24 °C). Data were low-pass-filtered at 5 kHz with a four-pole Bessel filter and sampled digitally at 25–100 kHz. In some experiments, capacitive and leakage currents were subtracted digitally using the P-P/4 procedure [4].

The pipette (internal) solution contained 10 mM NaCl, 110 mM CsCl, 20 mM tetra-ethylammonium (TEA)-Cl, 2.5 mM  $\text{MgCl}_2$ , 5 mM 4-2-hydroxyethyl-1-piperazine-ethanesulfonic acid (HEPES) and

5 mM ethylene glycol tetraacetic acid (EGTA). The pH of the pipette solution was adjusted to 7.0 with CsOH. Osmolarity was adjusted to 290 mosmol/kg with glucose. A part of the experiments were performed with the pipette solution containing phorbol 12-myristate 13-acetate (PMA), calphostin C, forskolin and H-89 (Sigma). For the pipette solution used in nystatin-perforated patch recordings, a stock solution containing 10mg/mL nystatin (Wako) was prepared and added to the pipette solution to final concentration of 500  $\mu\text{g/mL}$ . Patch clamp pipettes were made from borosilicate capillary by using a PP-83 puller (Narishige, Tokyo, Japan) and heat-polished with MF-83 microforge (Narishige). The DC resistance of patch electrodes was 1–1.5 M $\Omega$  for the conventional whole-cell patch and 3–5 M $\Omega$  for the nystatin-perforated patch, respectively.

The external solution contained 100 mM NaCl, 30 mM TEA-Cl, 5 mM CsCl, 1.8 mM CaCl<sub>2</sub>, 1 mM MgCl<sub>2</sub>, 0.1 mM CdCl<sub>2</sub>, 5 mM HEPES, 25 mM glucose, 5 mM 4-aminopyrimidine (4-AP). The pH of the external solution was adjusted to 7.4 with HCl. TEA-Cl and 4-AP were added to abolish K<sup>+</sup> currents and CdCl<sub>2</sub> was added to abolish Ca<sup>2+</sup> currents [4]. In addition, TTX (Sanko, Tokyo, Japan) was added to eliminate TTX-S Na<sup>+</sup> currents. Osmolarity was adjusted to 290 mosmol/kg with glucose. A part of the experiments were performed with the external solution containing PMA and forskolin (Sigma). Liquid junction potentials between pipette and external solutions were compensated by adjusting the zero current potential to the liquid junction potential. Only cells showing an adequate voltage and space clamp [11] were used.

When measuring ion channel kinetics, it generally take a considerable time to execute the protocol, since a sufficient recovery period for the channel must be allowed between each test pulse ( $V_T$ ). For various reasons, the amplitudes of Na<sup>+</sup> currents are not always constant during recording, e.g., due to run-down of the current or to instability of the seal condition. This can be checked by applying a control pulse ( $V_C$ ) before each  $V_T$ . To avoid a possible time-dependent fluctuation of the analysis,  $V_C$  to a fixed voltage as applied 15 s before  $V_T$  or conditioning pre-pulse ( $V_{PRE}$ ). The amplitude of the current ( $I_C$ ) evoked by  $V_C$  served as a calibrator. The results are given as mean  $\pm$  standard error of the mean (S.E.M.). Statistical significance of differences was determined using Wilcoxon  $t$ -test and Mann-Whitney  $U$ -test. Differences were considered significant if  $P < 0.05$ .

#### 4. Conclusions

The spontaneous augmentation of the Na<sub>v</sub>1.9 current was significantly suppressed by activation of PKA, whereas activation of PKA did not affect the voltage dependence of inactivation for the Na<sub>v</sub>1.9 current. On the contrary, the finding that activation of PKC can affect the voltage dependence of inactivation for Na<sub>v</sub>1.9 in the perforated patch recordings, where the augmentation does not occur, suggests that the effects of PMA are independent of the augmentation process. These results indicate that the spontaneous augmentation of Na<sub>v</sub>1.9 was regulated directly by PKA, and indirectly by PKC.

#### References

1. Chahine, M.; Ziane, R.; Vijayaragaban, K.; Okamura, Y. Regulation of Na<sub>v</sub> channels in sensory neurons. *Trends Pharmacol. Sci.* **2005**, *26*, 496–502.
2. Cummins, T.R.; Rush, A.M. Voltage-gated sodium channel blockers for the treatment of neuropathic pain. *Expert Rev. Neurother.* **2007**, *7*, 1597–612.

3. Elliot, A.A.; Elliot, J.R. Characterization of TTX-sensitive and TTX-resistant sodium currents in small cells from adult rat dorsal root ganglia. *J. Physiol.* **1993**, *463*, 39–56.
4. Ogata, N.; Tatebayashi, H. Kinetic analysis of two types of Na<sup>+</sup> channels in rat dorsal root ganglia. *J. Physiol.* **1993**, *466*, 9–37.
5. Akopian, A.N.; Souslova, V.; England, S.; Okuse, K.; Ogata, N.; Ure, J.; Smith, A.; Kerr, B.J.; McMahon, S.B.; Boyce, H.; Hill, R.; Stanfa, L.C.; Dickerson, A.H.; Wood, J.N. The tetrodotoxin-resistant sodium channel SNS has a specialized function in pain pathways. *Nat. Neurosci.* **1999**, *2*, 541–548.
6. Renganathan, M.; Cummins, T.R.; Waxman, S.G. Contribution of Nav1.8 sodium channels to action potential electrogenesis in DRG neurons. *J. Neurophysiol.* **2001**, *86*, 629–640.
7. Cummins, T.R.; Dib-Hajj, S.D.; Black, J.A.; Akopian, A.N.; Wood, J.N.; Waxman, S.G. A novel persistent tetrodotoxin-resistant sodium current in sns-null and wild-type small primary sensory neurons. *J. Neurosci.* **1999**, *19*, 1–6.
8. Dib-Hajj, S.D.; Tyrell, L.; Escayg, A.; Wood, P.M.; Meisler, M.H.; Waxman, S.G. Coding sequence, genomic organization, and conserved chromosomal localization of the mouse gene *Scn11a* encoding the sodium channel NaN. *Genomics* **1999**, *59*, 309–318.
9. Herzog, R.I.; Cummins, T.R.; Waxman, S.G. Persistent TTX-resistant Na<sup>+</sup> current affects resting potential and response to depolarization in stimulated spinal sensory neurons. *J. Neurophysiol.* **2001**, *86*, 1351–1364.
10. Rugiero, F.; Mistry, M.; Sage, D.; Black, J.A.; Waxman, S.G.; Crest, M.; Clere, N.; Delmas, P.; Gola, M. Selective expression of a persistent tetrodotoxin-resistant Na<sup>+</sup> current and Nav1.9 subunit in myenteric sensory neurons. *J. Neurosci.* **2003**, *23*, 2715–2725.
11. Maruyama, H.; Yamamoto, M.; Matsutomi, T.; Zheng, T.; Nakata, Y.; Wood, J.N.; Ogata, N. Electrophysiological characterization of the tetrodotoxin-resistant Na<sup>+</sup> channel, Nav1.9, in mouse dorsal root ganglion neurons. *Pflugers Arch.* **2004**, *449*, 76–87.
12. Coste, B.; Osorio, N.; Padilla, O.; Crest, M.; Delmas, P. Gating and modulation of presumptive Nav1.9 channels in enteric and spinal sensory neurons. *Mol. Cell. Neurosci.* **2004**, *26*, 123–134.
13. Matsutomi, T.; Nakamoto, C.; Zheng, T.; Kakimura, J.; Ogata, N. Multiple types of Na<sup>+</sup> currents mediate action potential electrogenesis in small neurons of mouse dorsal root ganglia. *Pflugers Arch.* **2006**, *453*, 83–96.
14. Lu, T.; Lee, H.C.; Kabat, J.A.; Shibata, E.F. Modulation of rat cardiac sodium channel by the stimulatory G protein  $\alpha$  subunit. *J. Physiol.* **1999**, *518*, 371–384.
15. Aley, K.O.; Messing, R.O.; Mochly-Rosen, D.; Levine, J.D. Chronic hypersensitivity for inflammatory nociceptor sensitization mediated by the epsilon isozyme of protein kinase C. *J. Neurosci.* **2000**, *20*, 4680–4685.
16. Deschênes, I.; Neyroud, N.; DiSilvestre, D.; Marbán, E.; Yue, D.T.; Tomaselli, G.F. Isoform-specific modulation of voltage-gated Na<sup>+</sup> channels by calmodulin. *Circ. Res.* **2002**, *90*, E49–E57.
17. Zheng, T.; Kakimura, J.; Matsutomi, T.; Nakamoto, C.; Ogata, N. Prostaglandin E<sub>2</sub> has no effect on two components of tetrodotoxin-resistant Na<sup>+</sup> current in mouse dorsal Root ganglion. *J. Pharmacol. Sci.* **2007**, *103*, 93–102.
18. Coggeshall, R.E.; Tate, S.; Carlton, S.M. Differential expression of tetrodotoxin resistant sodium channels Nav1.8 and Nav1.9 in normal and inflamed rats. *Neurosci. Lett.* **2004**, *355*, 45–48.

19. Murphy, B.J.; Rossie, S.; De Jongh, K.S.; Catterall, W.A. Identification of the sites of selective phosphorylation and dephosphorylation of the rat brain Na<sup>+</sup> channel  $\alpha$  subunit by cAMP-dependent protein kinase and phosphoprotein phosphatases. *J. Biol. Chem.* **1993**, *268*, 27355–27362.
20. Smith, R.D.; Goldin, A.L. Potentiation of rat brain sodium channel currents by PKA in *Xenopus* oocytes involves the I-II linker. *Am. J. Physiol. Cell. Physiol.* **2000**, *278*, C638–C645.
21. Cantrell, A.R.; Tibbs, V.C.; Yu, F.H.; Murphy, B.J.; Sharp, E.M.; Qu, Y.; Catterall, W.A.; Scheuer, T. Molecular mechanism of convergent regulation of brain Na<sup>+</sup> channels by protein kinase C and protein kinase A anchored to AKAP-15. *Mol. Cell. Neurosci.* **2002**, *21*, 63–80.
22. West, J.W.; Numann, R.; Murphy, B.J.; Scheuer, T.; Catterall, W.A. A phosphorylation site in the Na<sup>+</sup> channel required for modulation by protein kinase C. *Science* **1991**, *254*, 866–868.
23. Qu, Y.; Rogers, J.C.; Tanada, T.N.; Catterall, W.A.; Scheuer, T. Phosphorylation of S1505 in the cardiac Na<sup>+</sup> channel inactivation gate is required for modulation by protein kinase C. *J. Gen. Physiol.* **1996**, *108*, 375–379.
24. Li, M.; West, J.W.; Lay, Y.; Scheuer, T.; Catterall, W.A. Functional modulation of brain sodium channels by cAMP-dependent phosphorylation. *Neuron* **1992**, *8*, 1151–1159.
25. Numann, R.; Hauschka, S.D.; Catterall, W.A.; Scheuer, T. Modulation of skeletal muscle sodium channels in a satellite cell line by protein kinase C. *J. Neurosci.* **1994**, *14*, 4226–4236.
26. Numann, R.; Catterall, W.A.; Scheuer, T. Functional modulation of brain sodium channels by protein kinase C phosphorylation. *Science* **1991**, *254*, 115–118.
27. Kausalia, V.; Mohamed, B.; Mohamed, C. Modulation of Na<sub>v</sub>1.7 and Na<sub>v</sub>1.8 Peripheral Nerve Sodium Channels by Protein Kinase A and Protein Kinase C. *J. Neurophysiol.* **2004**, *91*, 1556–1569.
28. Baker, M.D.; Chandra, S.Y.; Ding, Y.; Waxman, S.G.; Wood, J.N. GTP-induced tetrodotoxin-resistant Na<sup>+</sup> current regulates excitability in mouse and rat small diameter sensory neurons. *J. Physiol.* **2003**, *548*, 373–382.
29. Baker, M.D. Protein kinase C mediates up-regulation of tetrodotoxin-resistant, persistent Na<sup>+</sup> current in rat and mouse sensory neurons. *J. Physiol.* **2005**, *567*, 851–867.
30. Chen, H.; Lei, J.; He, X.; Qu, F.; Wang, Y.; Wen, W.; You, H.; Arendt-Nielsen, L. Peripheral involvement of PKA and PKC in subcutaneous bee venom-induced persistent nociception, mechanical hyperalgesia, and inflammation in rats. *Pain* **2008**, *135*, 31–36.
31. Cunha, F.Q.; Teixeira, M.M.; Ferreira, S.H. Pharmacological modulation of secondary mediator systems - cyclic AMP and cyclic GMP - on inflammatory hyperalgesia. *Br. J. Pharmacol.* **1999**, *127*, 671–678.
32. Cunha, J.M.; Rae, G.A.; Ferreira, S.H.; Cunha, F.Q. Endothelins induce ETB receptor-mediated mechanical hypernociception in rat hindpaw: roles of cAMP and protein kinase C. *Eur. J. Pharmacol.* **2004**, *501*, 87–94.
33. Khasar, S.G.; Lin, Y.H.; Martin, A.; Dadgar, J.; McMahon, T.; Wang, D.; Hundle, B.; Aley, K.O.; Isenberg, W.; McCarter, G.; Green, P.G.; Hodge, C.W.; Levine, J.D.; Messing, R.O. A novel nociceptor signaling pathway revealed in protein kinase C $\epsilon$  mutant mice. *Neuron* **1999**, *24*, 253–260.

34. Martin, W.J.; Liu, H.; Wang, H.; Malmberg, A.B.; Basbaum, A.I. Inflammation-induced up-regulation of protein kinase C $\gamma$  immunoreactivity in rat spinal cord correlates with enhanced nociceptive processing. *Neuroscience* **1999**, *88*, 1267–1274.
35. Aley, K.O.; Martin, A.; McMahon, T.; Mok, J.; Levine, J.D.; Messing, R.O. Nociceptor sensitization by extracellular signal-regulated kinases. *J. Neurosci.* **2001**, *21*, 6933–6939.
36. Igwe, O.J.; Chronwall, B.M. Hyperalgesia induced by peripheral inflammation is mediated by protein kinase C  $\beta$ II isozyme in the rat spinal cord. *Neuroscience* **2001**, *104*, 875–890.
37. Priest, B.T.; Murphy, B.A.; Lindia, J.A.; Diaz, C.; Abbadie, C.; Ritter, A.M.; Liberator, P.; Iyer, L.M.; Kash, S.F.; Kohler, M.G.; Kaczorowski, G.J.; MacIntyre, D.E.; Martin, W.J. Contribution of the tetrodotoxin-resistant voltage-gated sodium channel Na $_v$ 1.9 to sensory transmission and nociceptive behavior. *Proc. Natl. Acad. Sci. USA* **2005**, *102*, 9382–9387.
38. Hamill, O.P.; Marty, A.; Neher, E.; Sakmann, B.; Sigworth, F.J. Improved patch-clamp techniques for high-resolution current recordings from cells and cell-free membrane patches. *Pflugers Arch.* **1981**, *391*, 85–100.
39. Horn, R.; Marty, A. Muscarinic activation of ionic currents measured by a new whole-cell recording method. *J. Gen. Physiol.* **1988**, *92*, 145–159.

© 2010 by the authors; licensee Molecular Diversity Preservation International, Basel, Switzerland. This article is an open-access article distributed under the terms and conditions of the Creative Commons Attribution license (<http://creativecommons.org/licenses/by/3.0/>).